Neonatal Neural Networks Predict Children Behavioral Profiles Later in Life

Chong-Yaw Wee,[1] Ta Anh Tuan,[1] Birit F. P. Broekman,[2,3] Min Yee Ong,[2]
Yap-Seng Chong,[2,4] Kenneth Kwek,[5] Lynette Shek,[6] Seang-Mei Saw,[7]
Peter D. Gluckman,[2] Marielle V. Fortier,[8] Michael J. Meaney,[2,9,10] and
Anqi Qiu[1,2]*

[1]*Department of Biomedical Engineering and Clinical Imaging Research Center, National University of Singapore, Singapore*
[2]*Singapore Institute for Clinical Sciences, Singapore*
[3]*Department of Psychological Medicine, Yong Loo Lin School of Medicine, National University of Singapore, National University Health System, Singapore*
[4]*Department of Obstetrics & Gynaecology, Yong Loo Lin School of Medicine, National University of Singapore, National University Health System, Singapore*
[5]*KK Women's and Children's Hospital, Singapore*
[6]*Yong Loo Lin School of Medicine, National University of Singapore, National University Health System, Singapore*
[7]*Saw Swee Hock School of Public Health, National University of Singapore, Singapore*
[8]*Department of Diagnostic and Interventional Imaging, KK Women's and Children's Hospital, Singapore (KKH)*
[9]*Ludmer Centre for Neuroinformatics and Mental Health, Douglas Mental Health University Institute, McGill University, Montréal, Canada*
[10]*Sackler Program for Epigenetics & Psychobiology at McGill University, Montréal, Canada*

◆ ▬▬▬▬▬▬▬▬▬▬▬▬▬▬▬▬▬▬▬▬ ◆
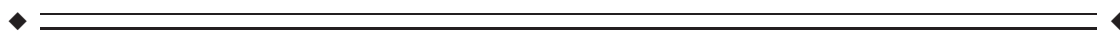
Abstract: This study aimed to examine heterogeneity of neonatal brain network and its prediction to child behaviors at 24 and 48 months of age. Diffusion tensor imaging (DTI) tractography was employed to construct brain anatomical network for 120 neonates. Clustering coefficients of individual structures were computed and used to classify neonates with similar brain anatomical networks into one group. Internalizing and externalizing behavioral problems were assessed using maternal reports of the Child Behavior Checklist (CBCL) at 24 and 48 months of age. The profile of CBCL externalizing and internalizing behaviors was then examined in the groups identified based on the neonatal brain network. Finally, support vector machine and canonical correlation analysis were used to identify brain structures whose clustering coefficients together significantly contribute the variation of the

behaviors at 24 and 48 months of age. Four meaningful groups were revealed based on the brain anatomical networks at birth. Moreover, the clustering coefficients of the brain regions that most contributed to this grouping of neonates were significantly associated with childhood internalizing and externalizing behaviors assessed at 24 and 48 months of age. Specially, the clustering coefficient of the right amygdala was associated with both internalizing and externalizing behaviors at 24 months of age, while the clustering coefficients of the right inferior frontal cortex and insula were associated with externalizing behaviors at 48 months of age. Our findings suggested that neural organization established during fetal development could to some extent predict individual differences in behavioral-emotional problems in early childhood. *Hum Brain Mapp 38:1362–1373, 2017.*   © 2016 **W**iley Periodicals, Inc.

INTRODUCTION

The quality of the materno-fetal environment influences subsequent risks for psychopathology in the offspring. Children born to more anxious mothers show increased risks for socio-emotional problems [O'Connor et al., 2003], attention deficit hyperactivity disorder (ADHD) [Van den Bergh and Marcoen, 2004], and anxiety [Clavarino et al., 2010]. Children of mothers with antenatal depression show increased internalizing and externalizing problems in childhood [Betts et al., 2014; Gentile, 2015] and are subsequently at a greater risk for depression [Pawlby et al., 2009]. These sustained impacts of the materno-fetal environment on the mental health of the offspring may suggest their influences on fetal neurodevelopment. Indeed, there is now considerable evidence for an association between antenatal maternal mental health and fetal brain development [Buss et al., 2012; Qiu et al., 2013; Rifkin-Graboi et al., 2013, 2015], including studies in which neuroimaging was performed in newborns. Such studies reveal that neonates born to mothers with a higher level of antenatal depressive symptoms show abnormal microstructure of the right amygdala compared with those born to mothers with a lower level of antenatal depressive symptoms [Rifkin-Graboi et al., 2013]. Antenatal maternal anxiety is associated with microstructure of the right insula in neonates, which in turn predicted socio-emotional problems of these children at 1 year of age [Rifkin-Graboi et al., 2015]. A meta-analysis of imaging studies on anxiety disorders revealed the insula and amygdala as the two most affected structures [Etkin and Wager, 2007], suggesting that vulnerability for affective disorders may, in part, be established during fetal development. Taken together, in utero insult during pregnancy may have consequences to the fetal development of the nervous system and such influences on the brain at the fetal stage could be the origin of the neurodevelopment for behavioral problems and neurodevelopmental disorders later in life.

While individual brain structures are linked to function, they are wired in compact and economical networks and easily transfer information in short and long distances to adapt to demands [Bullmore and Sporns, 2012]. Diffusion Tensor Imaging (DTI), an *in vivo* brain imaging technique, characterizes water diffusion within the brain tissue and is used to identify routes connecting different brain regions [Mori and Zhang, 2006], which thus reflect the organization and architecture of the neuroanatomical network. Research with both preterm and intrauterine growth restricted (IUGR) children suggests that altered neuroanatomical organization is associated with abnormal socio-emotional behaviors in infants [Ball et al., 2015; Batalle et al., 2012]. These inter-individual differences in neural structures and neuroanatomical networks underlying behavioral–emotional function may be established during fetal development. Given the evidence of the fetal brain development as a function of fetal exposure to adversity [Ghassabian et al., 2013; Qiu et al., 2013; Rifkin-Graboi et al., 2013, 2015; Schlotz et al., 2014], it remains unclear whether the heterogeneity in the neuroanatomical wiring architecture exists at birth and what is the prospective relation of this potential anatomical network heterogeneity with the variability of children's behaviors later in life.

In this study, we aimed to investigate the heterogeneity of the neuroanatomical network among full-term neonates and to understand to what extent the neuroanatomical network can explain the variation of internalizing and externalizing behaviors in the first 4 years of life. For this, we first examined the brain anatomical organization in full-term neonates at birth using DTI and tractography technique and then identified neonates with the similar neuroanatomical wiring organization using data-driven graph-based clustering algorithms, i.e., community detection and consensus clustering [Fair et al., 2012]. We then examined internalizing and externalizing behavioral profiles at 24 and 48 months of age in each group identified based on the neonatal neuroanatomical network. We employed support vector machine (SVM) to select brain regions whose anatomical organization was strongly associated with children behavior problems. The feature selection using SVM provides a great advantage on dimensionality reduction of the brain network measures, which hence facilitates multivariate analysis for linking the brain network measures

with the CBCL. We hypothesized that the heterogeneity of the neuroanatomical networks at birth can to certain extent reflect the variability of the behavioral development in early childhood. In particular, we expected that a set of brain regions and their structural organization might be more relevant to behavioral problems in the first 4 years of life than others. The outcomes of this study provide, to our knowledge, the direct link between the neonatal neuroanatomical wiring and behavior profiles in early childhood.

MATERIALS AND METHODS

Participants

One-hundred and eighty-nine infants of mothers who participated in the prospective Growing Up in Singapore Toward healthy Outcomes (GUSTO) birth cohort study [Soh et al., 2012] were recruited for neuroimaging. We included the 120 neonates who completed DTI scans (partly because DTI was acquired last), gestational age ≥37 weeks, birth weight ≥2,500 g, and a 5-minute APGAR score ≥9.

The GUSTO study was approved by the National Healthcare Group Domain Specific Review Board (NHG DSRB) and the Sing Health Centralized Institutional Review Board (CIRB). Written consent was obtained from mothers.

Child Behavior Checklist (CBCL)

Child internalizing and externalizing behavior problems were assessed with maternal reports using the Child Behavior Checklist (CBCL version1.5–5.0 years) [Achenbach, 1991] at 24 and 48 months. The CBCL consists of 99 items that report on emotional, behavioral and social difficulties. It uses a 3-point Likert scale with high reliability even in Singaporean [Rescorla et al., 2014]. The score for internalizing problems is derived from the emotionally reactive, anxious/depressed, somatic complaints, and withdrawn scales. The score for externalizing problems is the combination of the attention and aggressive behavioral problems scales. Raw scores were converted to age-standardized scores using T-scores, which were subsequently used in this study [Achenbach, 1991].

MRI Acquisition and Anatomical Network Analysis

Axial single-shot echo-planar diffusion weighted (DW) MRI scans (TR = 7,000 ms; TE = 56 ms; flip angle = 90°, FOV = 200 mm × 200 mm; matrix size = 256 × 256; 40–50 axial slices with 3.0 mm thickness; 19 diffusion directions with b = 600 sec/mm^2; 1 baseline image with b = 0 sec/mm^2) were acquired in infants at 5–14 days of age using a 1.5-Tesla GE scanner. The scans were acquired when subjects were sleeping in the scanner. No sedation was used

and precautions were taken to reduce exposure to the MRI scanner noise. A neonatologist was present during each scan. A pulse oximeter was used to monitor heart rate and oxygen saturation throughout the entire scans. The detailed image quality check procedure was previously reported [Qiu et al., 2013].

DWIs were analyzed based on the procedure shown in Figure 1A [Ratnarajah et al., 2013]. In brief, DWIs of each subject were first corrected for motion and eddy current distortion using affine transformation to the image without diffusion weighting. Using multivariate least-square fitting, six elements of the diffusion tensor were determined from which fractional anisotropy (FA) was calculated. The FA image and the image without diffusion weighting were then simultaneously aligned via affine and nonlinear large deformation diffeomorphic metric mapping transformations [Du et al., 2011] to those of the neonatal brain DTI atlas [Oishi et al., 2011] with manually labeled 32 cortical and sub-cortical structures per hemisphere. The reorientation scheme of diffusion tensor was performed using the preservation of principal direction (PPD) method, in which the reoriented tensor keeps its eigenvalues, yet its principal vector is transformed [Cao et al., 2005], to transform subjects' DTI to the atlas.

Whole-brain fiber tractography was performed using fiber assignment by continuous tracking (FACT) algorithm [Mori et al., 1999] with stopping criteria of FA <0.1 or fiber turning angle >70°. Based on the neonatal brain atlas [Oishi et al., 2011] and whole brain tractography, a 64 × 64 matrix was constructed to represent a brain anatomical network among the cortical and subcortical regions. The $(i, j)^{th}$ element in the matrix, denoting the connectivity strength between regions i and j, was computed by the number of fiber tracts connecting regions i and j normalized by the mean volume of the two regions. To eliminate brain connections due to noise effects of whole brain tractography, a non-parametric one-tailed sign test was performed on each element of the matrices across all the subjects to determine the connectivity between any two regions, i.e., the number of fiber tracts passing through regions i and j is larger than zero at a significance level of 0.05. A clustering coefficient of each brain region in the anatomical network was computed using Brain Connectivity Toolbox [Rubinov and Sporns, 2010] as the proportion of anatomical connections between the brain regions within its neighborhood divided by the number of connections that could possibly exist among them. The clustering coefficient of a brain region quantifies how close its neighbors are to being a clique. It ranges from 0 to 1. If every neighbor connected to a brain region is also connected to every other brain region within the neighborhood, the clustering coefficient of this brain region is 1. Previous studies suggested that the clustering coefficient is a more robust graph measure for classification as compared with brain connectivity itself or other graph measures, such as nodal betweenness centrality and nodal degree [Prasad et al.,
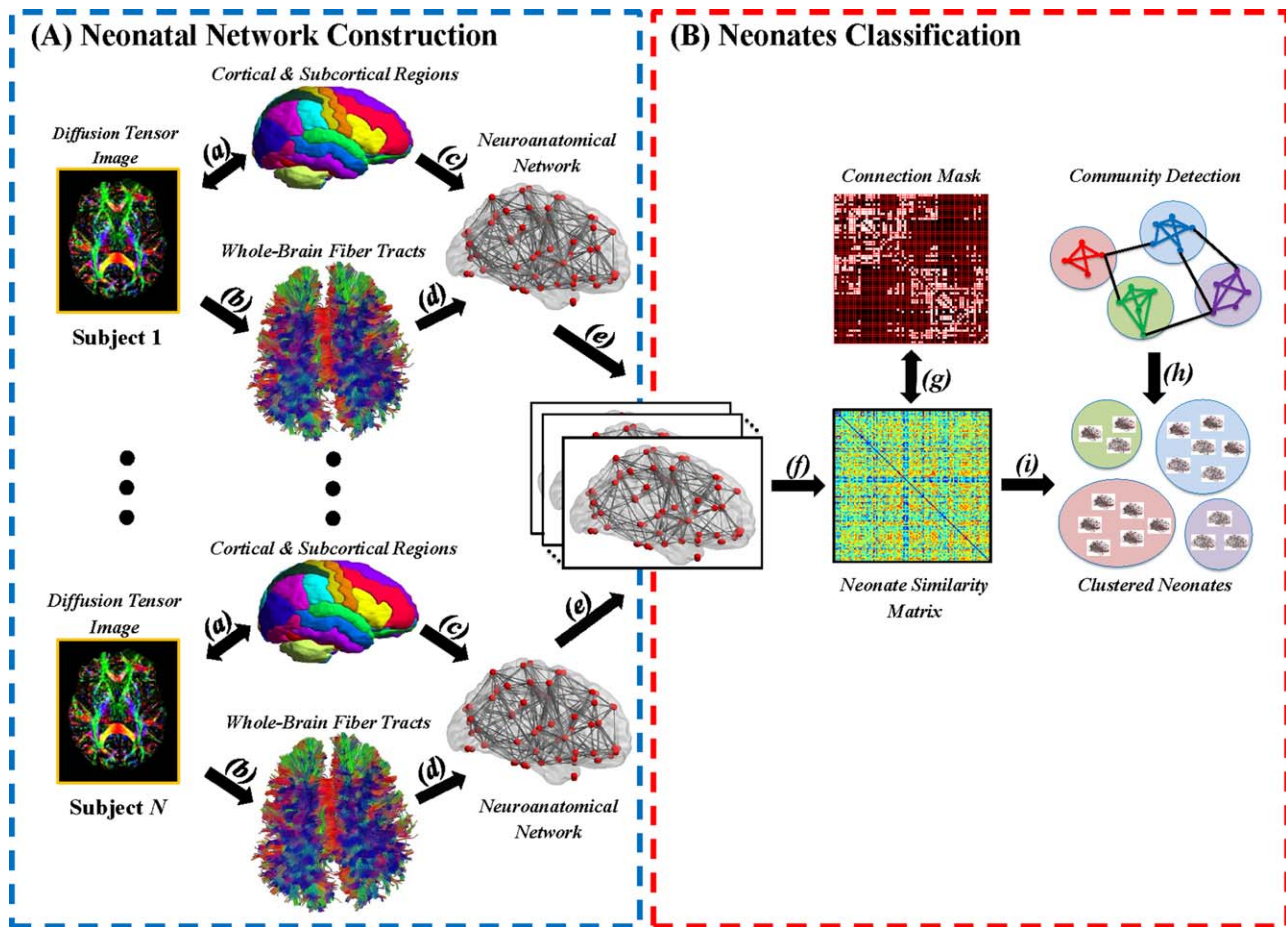
Figure 1.

A schematic diagram illustrates the major processes involved in (A) the construction of the neonatal brain anatomical networks, and (B) the classification of neonates via community detection technique. Note. (a) registration of diffusion tensor image (DTI) to the neonatal brain atlas; (b) whole brain tractography using DTI deterministic tractography; (c) the atlas parcellation; and (d) the anatomical network generated based on the whole brain tractography and atlas parcellation; (e) the determination of the existence of the anatomical connections between any two regions based on brain anatomical networks of all neonates; (f) the construction of similarity matrix using brain anatomical networks of all neonates; (g) trimming of the similarity matrix such that all subjects were connected to each other with at least one edge; (h, i) Louvain's community detection and consensus clustering. [Color figure can be viewed at wileyonlinelibrary.com]

2015; Wee et al., 2016]. Hence, this study employed the clustering coefficients as features for the following classification, where the clustering coefficients were standardized across all the brain regions.

Subject Classification Based on Anatomical Networks

A unified community detection and consensus partition framework was employed to classify subjects with similar anatomical networks into the same group. First, a similarity matrix was constructed with its $(i,j)^{th}$ element computed via Pearson's correlation of the clustering coefficients between the ith and j^{th} subjects. This similarity matrix was used to quantify the similarity of the anatomical networks among the subjects. Second, this similarity matrix was treated as a graph with each subject as a node and the Pearson's correlation coefficient of the clustering coefficients between the ith and j^{th} subjects as a weight of the $(i,j)^{th}$ edge. In this graph, many edges had low weights, suggesting a low probability of classifying the subjects connecting via these edges into one group. A maximum Pearson's correlation value ($r = 0.60$) was determined to trim the graph such that all subjects were connected to each other with at least one edge. Third,

community detection [Blondel et al., 2008] rearranged the nodes on the graph such that the nodes (or subjects) whose edges were with great weights were classified in one clique, while the nodes (or subjects) whose edges were with small weights were segregated into different cliques. The community detection achieved this by optimizing the segregation among identified subject cliques via maximizing Louvain's modularity, Q. A greater Q value indicates better separation among the subject groups. However, the community detection algorithm is nondeterministic in the sense that it may provide different classification results each time even though the same graph is given as its input. Fourth, a consensus partition procedure [Lancichinetti and Fortunato, 2012] was further used to overcome this issue of the community detection algorithm. A consensus matrix was constructed with its element represented the probability at which a pair of subjects were assigned to the same group based on 10,000 runs of community detection. The consensus matrix was trimmed to remove weak consensus less than 0.2 at which the classification of a pair of subjects in the same group was unlikely. Finally, the community detection was applied on this thresholded consensus matrix to assign subjects in different groups. The consensus partition procedure was repeated for several times to ensure that the same classification results were obtained. In addition, the consensus partition procedure was also repeated with various threshold values to trim the consensus matrix (0.20, 0.25, 0.30, 0.35) and showed that regardless this threshold value the consensus partition procedure consistently yielded the same classification results.

Next, the robustness of the subject classification result was evaluated by comparing how well the community detection can segregate the identified subject groups based on the aforementioned graph with that from random graphs with the same graph properties as that of the similarity matrix, including the number of nodes and edges, as well as weights of edges [Rubinov and Sporns, 2011]. This evaluation is crucial to ensure that the subject classification is unique and real as suggested by Reichardt and Bornholdt [2007]. Quantitatively, ten thousands random graphs were generated with the same number of nodes and edges, as well as weights of edges as that of the aforementioned similarity matrix and then applied the community detection to each graph to obtain the modularity Q-value. From these ten thousands random graphs, the null Q-distribution can be constructed. The robustness of the classification result was quantified as the percentage of Q-values from the random graphs greater than that of the graph obtained from our real brain data. Here, the Q-value obtained from our real brain data was the average Q-value derived from the aforementioned 10,000 runs of the community detection for the construction of the consensus matrix. If this is less than 5%, then the subject classification based on the neonatal brain networks is statistically robust. Furthermore, the confidence of the subject classification was quantified using the probability of each subject assigned to the same group based on the aforementioned 10,000 runs of community detection for the construction of the consensus matrix.

Statistical Analysis

A nested 10-fold cross-validation with linear support vector machine (SVM) was used to identify a subset of brain structures whose clustering coefficients best distinguish the subjects in the two groups with extreme values of CBCL scores. The linear SVM classifier based on the MATLAB version of the LIBSVM library [Chang and Lin, 2011] was adopted in this study. Figure S1 in the Supporting Information shows a schematic diagram of the nested 10-fold cross-validation procedure. In short, this nested 10-fold cross validation contained two layers, inner and outer layers. In the outer layer, the full set of subjects was randomly divided into 10 different sets with equal sample sizes; one was considered as a test set, and the remaining 9 sets were considered as a training set. In the inner layer, the subjects from the training set were further randomly divided into 10 different training subsets; again one was considered as a validation set and the remaining 9 subsets were considered as an inner training set. Based on the training set in the inner layer, the dimensionality of the features (in our case, clustering coefficients of 64 brain regions) was first reduced by minimizing the total relevance of each feature-feature pairs to achieve minimum redundancy and simultaneously maximizing the total relevance of each feature-class pairs to achieve maximum relevance condition [Peng et al., 2005]. An SVM-based recursive feature elimination (SVM-RFE) algorithm [Guyon et al., 2004] was then employed to determine a subset of features (brain structures) that optimizes the performance of the SVM classifier on the validation set. This reduction of feature dimensionality and SVM-RFE were repeated for 10 times in the inner layer. Once the optimal set of features was selected in the inner layer, it was then used as features to classify the testing set in the outer layer. This cross-validation procedure was repeated 10 times in the outer layer. Hence, this nested 10-fold cross validation procedure had total 100 validations and generated 100 different optimal subsets of brain structures for the SVM classification. The subject classification accuracy was also computed based on these 100 validations. Finally, we examined the distribution of the selection rate for all brain structures (see Fig. S2 in the Supporting Information) among the 100 validations and reported those with >65% of the selection rate as the important brain regions contributing to classifying the subjects in the two groups with extreme values of CBCL scores. This threshold was determined empirically. From Figure S2 in the Supporting Information, any value between 50% and 65% as threshold provides the same results on the selection of the brain regions.

TABLE I. Demographic characteristics of participants (N = 120)

Characteristic	Mean	SD	N	%
Gestational age (week)	40.1	1.2		
Birth weight (g)	3,258.7	374.7		
Sex (male)			64	53.3
Ethnicity				
Chinese			52	43.3
Malay			50	41.7
Indian			18	15.0
Internalizing score at 24 months	50.43	12.04	80	
Externalizing score at 24 months	48.64	9.46	80	
Internalizing score at 48 months	49.16	11.54	72	
Externalizing score at 48 months	44.65	10.30	72	

SD, standard deviation.

To investigate how a set of the selected brain regions contributes to the variation of CBCL internalizing or externalizing problems, a multivariate canonical correlation analysis (CCA) was used to examine the joint contribution of clustering coefficients of these important brain regions to CBCL internalizing or externalizing scores among all the subjects at each time point. Note that a standardized version of clustering coefficient (z-score) was used in CCA. These four CCA were corrected for multiple comparisons using Bonferroni correction. Only for the interpretation of the results derived from CCA, pairwise Pearson's correlation analysis was performed between clustering coefficients of these brain regions and CBCL scores that showed the significance from the canonical correlation analysis.
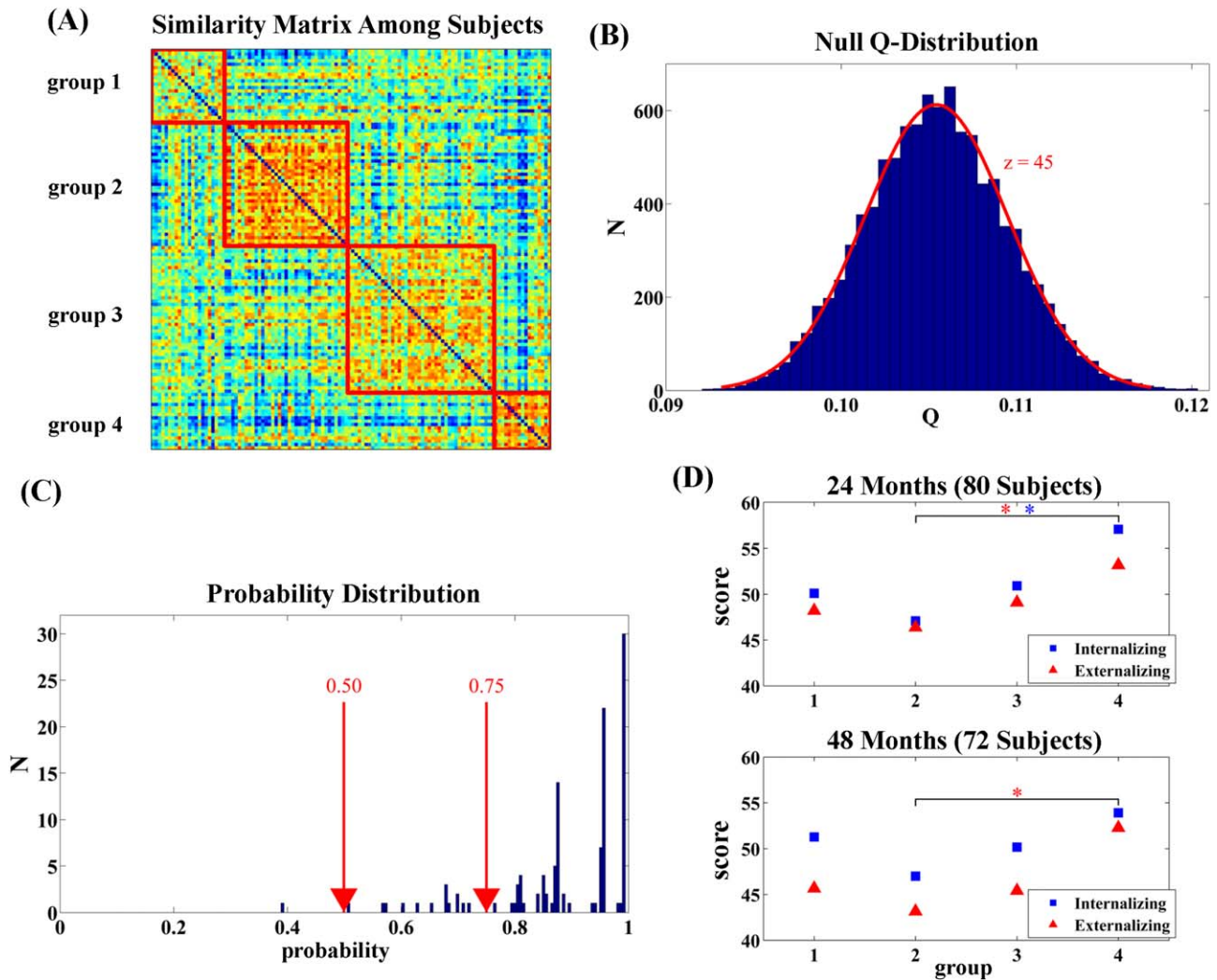
RESULTS

This study included DTI data of 120 neonates. Demographic characteristics of the neonates including gestational age, birth weight, gender and ethnicity, as well as their CBCL internalizing and externalizing scores at 24 and 48 months are provided in Table I. Among these subjects, the mothers of 80 and 72 subjects answered the CBCL at 24 and 48 months, respectively.

Distinct patterns of neonatal neuroanatomical networks were identified, resulting four groups with size of 22, 37, 44, and 17, respectively. The non-random nature of the grouping pattern in Figure 2A was revealed by the modularity Q-value ($Q = 0.293$), which was significantly ($P < 0.001$) greater than those of the 10,000 randomly-generated similarity matrices (Fig. 2B). Moreover, more than 87% of the neonates were assigned to the same group with a probability greater than 0.75 (Fig. 2C). Only one neonate had a probability less than 0.5.

As illustrated in Figure 2D, group 2 showed the lowest internalizing and externalizing scores at both ages among the four groups, while group 4 had the highest scores and the scores of groups 1 and 3 fell between groups 2 and 4. There was no group difference among the four groups in the internalizing problem score at 24 months (Welch

ANOVA $t_{34.6} = 1.750$, $P = 0.17$) but a trend of significance for the internalizing problem score at 48 months (Welch ANOVA $t_{33.6} = 2.720$, $P = 0.06$). In contrast, a trend of significant group difference was observed in the externalizing problem score at 24 months (Welch ANOVA $t_{38.4} = 2.480$, $P = 0.08$) but no significant group difference was in the externalizing problem score at 48 months (Welch $t_{31.1} = 1.610$, $P = 0.21$). Since manifestations of psychopathology are less differentiated in infancy and early childhood [Sonuga-Barke et al., 1997] and our sample was from a general population, we only expected significant differences in the CBCL between the two groups (groups 2 and 4) with extreme values of CBCL behavioral scores. Indeed, neonates from group 4 experienced significantly more externalizing and internalizing behavioral problems than those from group 2 at 24 months of age (internalizing: Welch $t_{20.9} = 2.323$, $P = 0.03$; externalizing: Welch $t_{31} = 2.642$, $P = 0.01$). However, only the externalizing behavioral problems remained significant at 48 months of age (Welch $t_{18.1} = -2.496$, $P = 0.02$) while internalizing behavioral problems were marginally significant (Welch $t_{21.4} = -1.825$, $P = 0.08$).

SVM distinguished neonates of groups 2 and 4 at relatively high classification accuracy of 89.4% (sensitive = 0.954, specificity = 0.765). Brain regions that most frequently contributed to the discrimination of neonates in groups 2 and 4 were bilateral amygdala, left superior temporal gyrus, right insular cortex, right inferior frontal gyrus, left inferior temporal gyrus, left middle occipital gyrus, and right medial fronto-orbital gyrus. CCA revealed that the clustering coefficients of these structures were highly correlated with internalizing ($\chi^2 = 20.51$, df = 8, $P = 0.009$) and externalizing scores ($\chi^2 = 19.18$, df = 8, $P = 0.01$) at 24 months, which were also survived for multiple comparisons. Nevertheless, CCA revealed that the clustering coefficients of these structures were highly correlated with externalizing score at 48 months ($\chi^2 = 17.09$, df = 8, $P = 0.03$; not survived for multiple comparisons), but not with internalizing scores at 48 months ($\chi^2 = 11.89$, df = 8, $P = 0.16$). Only for visualization purpose, the association between CBCL scores and individual brain structures that most contributed to the discrimination of neonatal neural networks (Table II and Fig. 3) were further examined and revealed that the clustering coefficient of the right amygdala was significantly correlated with both internalizing and externalizing behavioral problems at 24 months of age, suggesting that a greater level of clustering anatomical connections between the right amygdala and the rest of the brain into tightly connected neighborhoods was associated with less internalizing and externalizing problems in children at 24 months of age. The clustering coefficients of the right inferior frontal gyrus and right insula were significantly correlated with externalizing behavioral problems of 48 months (Table II), suggesting that a less level of clustering anatomical connections of the right inferior frontal gyrus and right insula with the rest of the brain into tightly connected neighborhoods

Figure 2.

Clustering results. Panel (A) shows the similarity matrix of the neuroanatomical networks among all the neonates in this study and its clustering pattern. Panel (B) illustrates the null Q-distribution that were generated based on 10,000 random graphs with the same graph properties, such as degree, node, weight, as that shown in panel (A). The Q-value in panel (A) is at 45 standard deviations from the mean of the null Q-distribution ($z = 45$). Panel (C) shows the probability distribution, indicating the chance of each neonate consistently assigned to the same group when community detection was reran for 10,000 times. Panel (D) shows the profiles of 24-month (top) and 48-month (bottom) internalizing and externalizing behaviors in the four groups shown in panel (A). * indicates significant group differences at a significance level of 0.05. [Color figure can be viewed at wileyonlinelibrary.com]

was associated with less externalizing problems in children at 48 months of age. Likewise, the clustering coefficient of the left superior temporal gyrus was correlated with the internalizing score at 24 months (Table II), suggesting that a less level of clustering anatomical connections between the left superior temporal gyrus and the rest of the brain into tightly connected neighborhoods was associated with less internalizing and problems in children at 24 months of age. Table S1 in the Supporting Information provides additional correlation results after removing "extreme" cases (see Fig. S3 in the Supporting Information), suggesting similar trends of the aforementioned association.

DISCUSSION

This study was, to our knowledge, the first study to describe inter-individual variation in neuroanatomical

TABLE II. Pearson's correlation of clustering coefficients of individual brain structures with internalizing and externalizing scores

	Internalizing 24-month r	Externalizing	
Region		24-month r	48-month r
Left Amygdala (LA)	0.117	0.121	0.140
Right Amygdala (RA)	**−0.270**[a]	**−0.296****	−0.186
Left Superior Temporal Gyrus (LSTG)	**0.250**[a]	0.200	0.221
Right Insular Cortex (RIC)	−0.169	−0.170	**0.316****
Right Inferior Frontal Gyrus (RIFG)	0.123	0.146	**0.262**[a]
Left Inferior Temporal Gyrus (LITG)	−0.107	−0.023	−0.001
Left Middle Occipital Gyrus (LMOG)	−0.122	−0.123	−0.037
Right Medial Fronto-Orbital Gyrus (RMFOG)	0.105	−0.014	0.217

Note. Only the time points with significant correlation between brain measures and behavioral problem scores in canonical correlation analysis are shown above.
[a]$P < 0.05$; ** $P < 0.01$.

networks at birth in relation to subsequent childhood behaviors. The results of the graph-based clustering analysis revealed meaningful neurodevelopment subgroups based on network connections at birth. Moreover, the clustering coefficients of the brain regions that most contributed to the mathematical grouping of neonates were significantly associated with childhood internalizing and externalizing behaviors assessed at 24 and 48 months of age. Specially, the clustering coefficient of the right amygdala predicted both internalizing and externalizing behaviors at 24 months of age, while the clustering coefficients of the right inferior frontal cortex and insula predicted externalizing behavior at 48 months of age. Our findings suggested that neural organization established during fetal development was associated with individual differences in behavioral-emotional problems in early childhood. Our findings further showed a stronger association between cortical brain nodes (i.e., the insula, and the inferior frontal gyrus) at birth and behavioral-emotional function at 48 than at 24 months, which was consistent with an increasingly greater importance of cortical structures over the course of postnatal development. Nevertheless, it was important to note that the relevant variation in cortical connections was established over fetal development and apparent at birth.

Brain anatomical organization was variable across full-term neonates and significantly associated with behavioral-emotional function in childhood. The link to both internalizing and externalizing behavioral patterns is not surprising since manifestations of psychopathology are less differentiated in childhood and often comorbid [Sonuga-Barke et al., 1997]. Our findings were consistent with previous reports of the relationship between the brain anatomical organization and neurodevelopmental outcomes in preterm or intrauterine growth-restricted infants [Ball et al., 2015; Batalle et al., 2012]. Altered brain network topology in 1-year-old infants born small for gestational age is associated with abnormal socio-emotional and

adaptive behaviors measured by the Bayley's Scale for Infant and Toddler Development instrument at two years of age [Batalle et al., 2012]. Cortico-thalamic structural connectivity of preterm infants at term-equivalent age is correlated with cognitive scores at two years of age [Ball et al., 2015]. The results of the current study underscore the long-term importance of variation in fetal brain development even in full-term, healthy neonates.

The clustering coefficient of the right amygdala at birth was associated with both internalizing and externalizing behaviors at 24 months of age. The amygdala is an evolutionarily primitive brain region and is one of the earliest developing brain structures [Uematsu et al., 2012]. Buss et al. [2012] used a prospective, longitudinal study to show an association between antenatal maternal cortisol levels and the right amygdala volume at 7 years of age. Moreover, a higher maternal cortisol level in gestation was associated with emotional problems and this association was mediated, in part, by the amygdala volume. This finding was also consistent with our previous study showing that antenatal maternal emotional well-being is associated with abnormal microstructure of the right amygdala at birth [Rifkin-Graboi et al., 2013].

Imaging studies of the antenatal origins of variation in amygdala structure emphasize effects in the right hemisphere, which is associated with the processing of threat. Stress-induction procedures revealed greater activation in the right amygdala and increased connectivity between the right amygdala and the midbrain [Van Marle et al., 2009]. Functional imaging studies in humans show the involvement of the right amygdala in mood disorders, and in the processing of emotionally negative information and the accompanying stress responses [Hamilton and Gotlib, 2008; Pruessner et al., 2008]. Moreover, decreased functional connectivity between the amygdala and posterior insula is associated with increased behavioral and emotion dysregulation in youth [Bebko et al., 2015]. And abnormal amygdala activation and connectivity were observed in
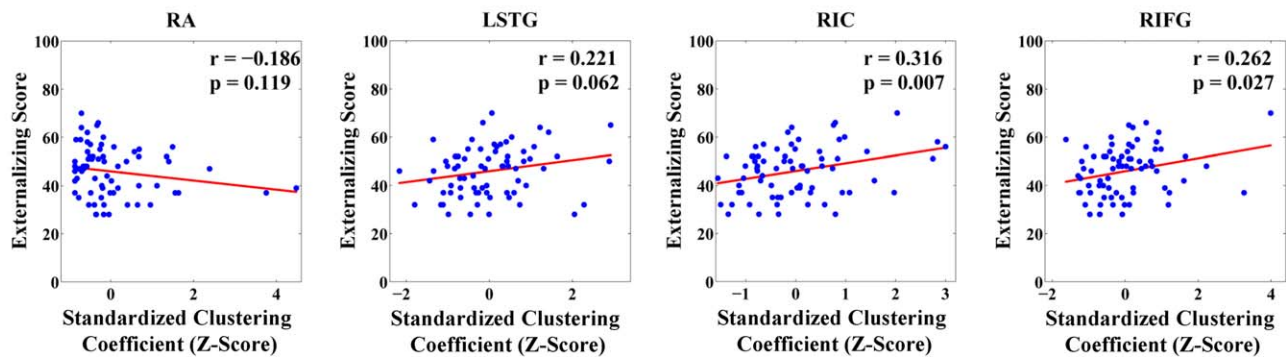
(A) Internalizing Behavioral Score (24 Months)
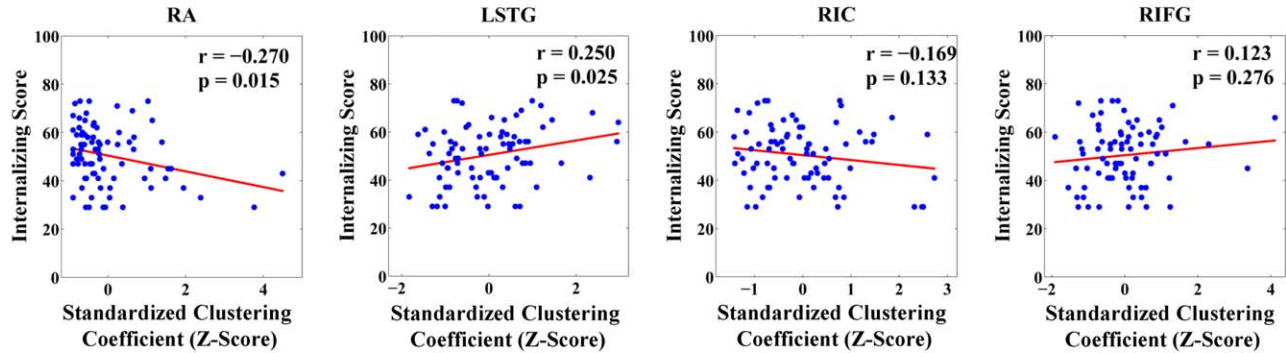
(B) Externalizing Behavioral Score (24 Months)
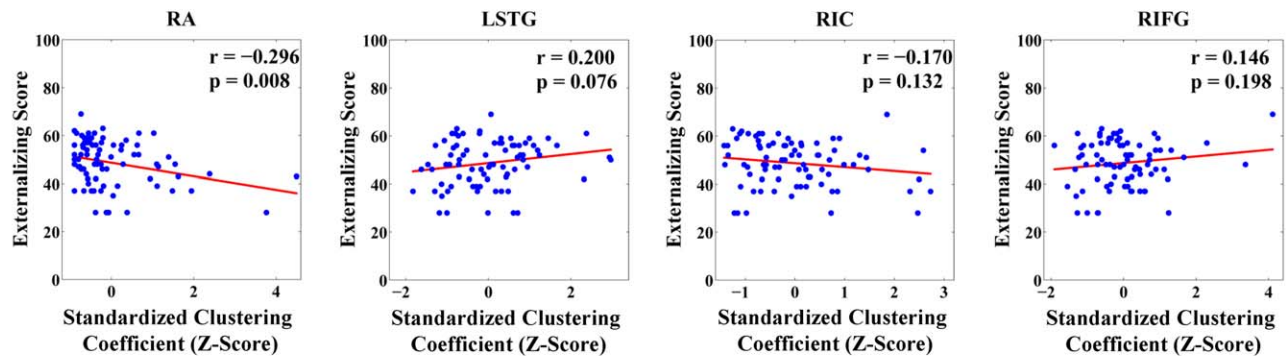
(C) Externalizing Behavioral Score (48 Months)

Figure 3.

Scatter plots of internalizing and externalizing scores with standardized clustering coefficients of individual brain structures. Panels (A, B, C) show the scatter plots for the internalizing and externalizing behavioral scores at 24 months of age and the externalizing behavioral score at 48 months of age, respectively. Abbreviations: RA, right amygdala; LSTG, left superior temporal gyrus; RIC, right insula; RIFG, right inferior frontal gyrus. [Color figure can be viewed at wileyonlinelibrary.com]

adolescents with ADHD [Posner et al., 2011]. Taken together, there are indications that right amygdala circuitry could be one of likely neural bases to various behavioral and emotional problems in early life.

Our findings suggested that the anatomical organization of distinct brain regions at birth can potentially encode the temporal patterns of behavioral development in early childhood. Sensory-related regions, such as the left

superior temporal gyrus and right amygdala, were strongly associated with internalizing and externalizing behaviors at 24 months. In contrast, brain regions related to higher-level behavioral–emotional processing, such as the right insula and inferior frontal cortex, were strongly associated with 48-month externalizing behaviors. Microstructure of the right insula at birth predicted socio-emotional problems assessed using Infant Toddler Social Emotional Assessment (ITSEA) at one year of age [Rifkin-Graboi et al., 2015]. Disrupted functional connectivity of the right insula has been found in children with conduct disorder [Fairchild et al., 2014; Michalska et al., 2015]. Functional MRI studies also suggest the involvement of the right inferior frontal gyrus in response inhibition [Hampshire et al., 2010]. Adolescents with ADHD show reduced brain activation in the right inferior frontal cortex during motor response inhibition [Rubia et al., 2005] and boys with ADHD show decreased connectivity in the right inferior frontal cortex as compared with typically developing boys [Zang et al., 2007].

There are several limitations of this study. The white matter in the neonatal brain is largely unmyelinated and hence has low diffusion anisotropy. This could cause potential termination of fiber tracking in deterministic tractography in the periphery white matter region. To overcome this issue, our study employed the neonatal brain atlas [Oishi et al., 2011] in which the cortical parcellation incorporates the corresponding periphery white matter region. Furthermore, to ensure reliable tractography results, we employed the FACT algorithm [Mori et al., 1999], one of the most validated tractographic approaches in infant studies, to perform whole-brain fiber tractography. Dubois et al. [2006] has demonstrated that the FACT algorithm can tract most of the main fibers despite low anisotropy of the infant white matter. To further enhance the tractography results, we used a FA threshold of 0.1, which is lower than that used in adults studies, and preserved only those tracts that passing through the deep white matter regions. Our tractography results were comparable to those presented in Dubois et al. [2006]. Nevertheless, this study reflects the novel use of computational approaches to examine the association between brain organization at birth and later emotional–behavioral function. As such, the results merit replication and extension with complimentary approach, both of which will become feasible with the emerging emphasis on neuroimaging of normal children.

CONCLUSION

There is now considerable focus on the important of the quality of fetal growth and development for later function, including mental health. A previously unmet assumption is that individual differences established during fetal neurodevelopment are functionally related to emotional and behavioral function in childhood. Our study directly addressed this issue and provided novel evidence that the variability of the brain anatomical organization at birth predicted internalizing and externalizing behaviors in early childhood, suggesting that fetal brain development plays a crucial role in behavioral development later in life.

REFERENCES

Achenbach TM (1991): Integrative Guide for the 1991 CBCL/4-18, Ysr, and TRF Profiles. Burlington: Department of Psychiatry, University of Vermont.

Ball G, Pazderova L, Chew A, Tusor N, Merchant N, Arichi T, Allsop JM, Cowan FM, Edwards AD, Counsell SJ (2015): Thalamocortical connectivity predicts cognition in children born preterm. Cereb Cortex 25:4310–4318.

Batalle D, Eixarch E, Figueras F, Muñoz-Moreno E, Bargallo N, Illa M, Acosta-Rojas R, Amat-Roldan I, Gratacos E (2012): Altered small-world topology of structural brain networks in infants with intrauterine growth restriction and its association with later neurodevelopmental outcome. Neuroimage 60: 1352–1366.

Bebko G, Bertocci M, Chase H, Dwojak A, Bonar L, Almeida J, Perlman SB, Versace A, Schirda C, Travis M, Gill MK, Demeter C, Diwadkar V, Sunshine J, Holland S, Kowatch R, Birmaher B, Axelson D, Horwitz S, Frazier T, Arnold LE, Fristad M, Youngstrom E, Findling R, Phillips ML (2015): Decreased amygdala–insula resting state connectivity in

behaviorally and emotionally dysregulated youth. Psychiatry Res 231:77–86.

Betts KS, Williams GM, Najman JM, Alati R (2014): Maternal depressive, anxious, and stress symptoms during pregnancy predict internalizing problems in adolescence. Depress Anxiety 31:9–18.

Blondel VD, Guillaume J-L, Lambiotte R, Lefebvre E (2008): Fast unfolding of communities in large networks. J Stat Mech: Theory Exp 2008:P10008.

Bullmore E, Sporns O (2012): The economy of brain network organization. Nat Rev Neurosci 13:336–349.

Buss C, Davis EP, Shahbaba B, Pruessner JC, Head K, Sandman CA (2012): Maternal cortisol over the course of pregnancy and subsequent child amygdala and hippocampus volumes and affective problems. Proc Natl Acad Sci U S A 109:E1312–E1319.

Cao Y, Miller MI, Winslow RL, Younes L (2005): Large deformation diffeomorphic metric mapping of vector fields. IEEE Trans Med Imaging 24:1216–1230.

Chang CC, Lin CJ (2011): LIBSVM: A library for support vector machines. ACM TIST 2:27:1–27.

Clavarino AM, Mamun AA, O'Callaghan M, Aird R, Bor W, O'Callaghan F, Williams GM, Marrington S, Najman JM, Alati R (2010): Maternal anxiety and attention problems in children at 5 and 14 years. J Atten Disord 13:658–667.

Du J, Younes L, Qiu A (2011): Whole brain diffeomorphic metric mapping via integration of sulcal and gyral curves, cortical surfaces, and images. Neuroimage 56:162–173.

Dubois J, Hertz-Pannier L, Dehaene-Lambertz G, Cointepas Y, Le Bihan D (2006): Assessment of the early organization and maturation of infants' cerebral white matter fiber bundles: A feasibility study using quantitative diffusion tensor imaging and tractography. Neuroimage 30:1121–1132.

Etkin A, Wager TD (2007): Functional neuroimaging of anxiety: A meta-analysis of emotional processing in PTSD, social anxiety disorder, and specific phobia. Am J Psychiatry 164:1476–1488.

Fair DA, Bathula D, Nikolas MA, Nigg JT (2012): Distinct neuropsychological subgroups in typically developing youth inform heterogeneity in children with ADHD. Proc Natl Acad Sci U S A 109:6769–6774.

Fairchild G, Hagan CC, Passamonti L, Walsh ND, Goodyer IM, Calder AJ (2014): Atypical neural responses during face processing in female adolescents with conduct disorder. J Am Acad Child Adolesc Psychiatry 53:677–687.e5.

Gentile S (2015): Untreated depression during pregnancy: Short- and long-term effects in offspring. A systematic review. Neuroscience S0306-4522:811–818.

Ghassabian A, Herba CM, Roza SJ, Govaert P, Schenk JJ, Jaddoe VW, Hofman A, White T, Verhulst FC, Tiemeier H (2013): Infant brain structures, executive function, and attention deficit/hyperactivity problems at preschool age. A prospective study. J Child Psychol Psychiatry 54:96–104.

Guyon I, Weston J, Barnhill S, Vapnik V (2004): Gene selection for cancer classification using support vector machines. Mach Learn 46:389–422.

Hamilton JP, Gotlib IH (2008): Neural substrates of increased memory sensitivity for negative stimuli in major depression. Biol Psychiatry 63:1155–1162.

Hampshire A, Chamberlain SR, Monti MM, Duncan J, Owen AM (2010): The role of the right inferior frontal gyrus: Inhibition and attentional control. Neuroimage 50:1313–1319.

Lancichinetti A, Fortunato S (2012): Consensus clustering in complex networks. Sci Rep 2:336.

Michalska KJ, Zeffiro TA, Decety J (2015): Brain response to viewing others being harmed in children with conduct disorder symptoms. J Child Psychol Psychiatry 57:510–519.

Mori S, Zhang J (2006): Principles of diffusion tensor imaging and its applications to basic neuroscience research. Neuron 51:527–539.

Mori S, Crain BJ, Chacko VP, van Zijl PC (1999): Three-dimensional tracking of axonal projections in the brain by magnetic resonance imaging. Ann Neurol 47:265–269.

O'Connor TG, Heron J, Golding J, Glover V, ALSPAC Study Team (2003): Maternal antenatal anxiety and behavioural/emotional problems in children: A test of a programming hypothesis. J Child Psychol Psychiatry 44:1025–1036.

Oishi K, Mori S, Donohue PK, Ernst T, Anderson L, Buchthal S, Faria A, Jiang H, Li X, Miller MI, van Zijl PC, Chang L (2011): Multi-contrast human neonatal brain atlas: Application to normal neonate development analysis. Neuroimage 56:8–20.

Pawlby S, Hay DF, Sharp D, Waters CS, O'Keane V (2009): Antenatal depression predicts depression in adolescent offspring: Prospective longitudinal community-based study. J Affect Disord 113:236–243.

Peng H, Long F, Ding C (2005): Feature selection based on mutual information: Criteria of max-dependency, max-relevance, and min-redundancy. IEEE Trans Pattern Anal Mach Intell 27:1226–1285.

Posner J, Nagel BJ, Maia TV, Mechling A, Oh M, Wang Z, Peterson BS (2011): Abnormal amygdalar activation and connectivity in adolescents with attention-deficit/hyperactivity disorder. J Am Acad Child Adolesc Psychiatry 50:828–837.e3.

Prasad G, Joshi SH, Nir TM, Toga AW, Thompson PM, for the Alzheimer's Disease Neuroimaging I (2015): Brain connectivity and novel network measures for Alzheimer's disease classification. Neurobiol Aging 36:S121–S131.

Pruessner JC, Dedovic K, Khalili-Mahani N, Engert V, Pruessner M, Buss C, Renwick R, Dagher A, Meaney MJ, Lupien S (2008): Deactivation of the limbic system during acute psychosocial stress: Evidence from positron emission tomography and functional magnetic resonance imaging studies. Biol Psychiatry 63:234–240.

Qiu A, Rifkin-Graboi A, Chen H, Chong YS, Kwek K, Gluckman PD, Fortier MV, Meaney MJ (2013): Maternal anxiety and infants' hippocampal development: Timing matters. Transl Psychiatry 3:e306.

Ratnarajah N, Rifkin-Graboi A, Fortier MV, Chong YS, Kwek K, Saw S-M, Godfrey KM, Gluckman PD, Meaney MJ, Qiu A (2013): Structural connectivity asymmetry in the neonatal brain. Neuroimage 75:187–194.

Reichardt J, Bornholdt S (2007): Partitioning and modularity of graphs with arbitrary degree distribution. Phys Rev E 76:(1):015102.

Rescorla LA, Bochicchio L, Achenbach TM, Ivanova MY, Almqvist F, Begovac I, Bilenberg N, Bird H, Dobrean A, Erol N, Fombonne E, Fonseca A, Frigerio A, Fung DS, Lambert MC, Leung PW, Liu X, Markovic I, Markovic J, Minaei A, Ooi YP, Roussos A, Rudan V, Simsek Z, van der Ende J, Weintraub S, Wolanczyk T, Woo B, Weiss B, Weisz J, Zukauskiene R, Verhulst FC (2014): Parent-teacher agreement on children's problems in 21 societies. J Clin Child Adolesc Psychol 43:627–642.

Rifkin-Graboi A, Bai J, Chen H, Hameed WB, Sim LW, Tint MT, Leutscher-Broekman B, Chong YS, Gluckman PD, Fortier MV, Meaney MJ, Qiu A (2013): Prenatal maternal depression

associates with microstructure of right amygdala in neonates at birth. Biol Psychiatry 74:837–844.

Rifkin-Graboi A, Meaney MJ, Chen H, Bai J, Hameed WB, Tint MT, Broekman BF, Chong YS, Gluckman PD, Fortier MV, Qiu A (2015): Antenatal maternal anxiety predicts variations in neural structures implicated in anxiety disorders in newborns. J Am Acad Child Adolesc Psychiatry 54:313–321.

Rubia K, Smith AB, Brammer MJ, Toone B, Taylor E (2005): Abnormal brain activation during inhibition and error detection in medication-naive adolescents with ADHD. Am J Psychiatry 162:1067–1075.

Rubinov M, Sporns O (2010): Complex network measures of brain connectivity: Uses and interpretations. Neuroimage 52: 1059–1069.

Rubinov M, Sporns O (2011): Weight-conserving characterization of complex functional brain networks. Neuroimage 56: 2068–2079.

Schlotz W, Godfrey KM, Phillips DI (2014): Prenatal origins of temperament: Fetal growth, brain structure, and inhibitory control in adolescence. PLoS ONE 9:e96715.

Soh SE, Lee SSM, Hoon SW, Tan MY, Goh A, Lee BW, Shek LP-C, Teoh OH, Kwek K, Saw SM, Godfrey K, Chong YS, Gluckman P, van Bever HPS (2012): The methodology of the GUSTO cohort study: A novel approach in studying pediatric allergy. Asia Pac Allergy 2:144–148.

Sonuga-Barke EJS, Thompson M, Stevenson J, Viney D (1997): Patterns of behaviour problems among pre-school children. Psychol Med 27:909–918.

Uematsu A, Matsui M, Tanaka C, Takahashi T, Noguchi K, Suzuki M, Nishijo H (2012): Developmental trajectories of amygdala and hippocampus from infancy to early adulthood in healthy individuals. PLoS ONE 7:e46970.

Van den Bergh BR, Marcoen A (2004): High antenatal maternal anxiety is related to ADHD symptoms, externalizing problems, and anxiety in 8- and 9-year-olds. Child Dev 75:1085–1097.

Van Marle HJ, Hermans EJ, Qin S, Fernandez G (2009): From specificity to sensitivity: How acute stress affects amygdala processing of biologically salient stimuli. Biol Psychiatry 66: 649–655.

Wee C-Y, Yang S, Yap P-T, Shen D (2016): Sparse temporally dynamic resting-state functional connectivity networks for early MCI identification. Brain Imaging Behav 10:342–356.

Zang YF, He Y, Zhu CZ, Cao QJ, Sui MQ, Liang M, Tian LX, Jiang TZ, Wang YF (2007): Altered baseline brain activity in children with ADHD revealed by resting-state functional MRI. Brain Dev 29:83–91.